Miniaturized Spoof Surface Plasmon Polaritons Low-Pass Filter With a Novel Transition Structure

Lili Wang, Xueqi Cui, Hailong Yang, Zhonghong Du, and Yuchen Zhao

***Abstract*— In this letter, a miniaturized spoof surface plasmon polaritons (SSPPs) low-pass filter with a novel transition structure is proposed. The novel transition structure is designed by two rectangular strips with an inclination of 17° and right-angled triangle patches. In this letter, we analyzed the normal and azimuthal components of the electric field perpendicular to the plane of the filter at different locations, verifying the effectiveness of the transitional structure. Besides, efficient conversion between quasi-transverse electromagnetic (TEM) waves and transverse magnetic (TM) polarized SSPPs waves are achieved by loading the novel transition structures. The designed filter can suppress unnecessary radiation loss and increase transmission efficiency. More importantly, the filter size is 47.52 mm × 7.47 mm and its length is reduced by at least 61% compared with the other low-pass filters with the same cutoff frequency. This letter has promoted the development and application of SSPPs low-pass filter and related equipment in microwave frequencies.**

***Index Terms*— Miniaturized low pass filter, novel transition structures, surface plasmons.**

I. Introduction

SURFACE plasmon polaritons (SPPs) are electromagnetic waves that propagate along the interface between metal and dielectric in an optical regime [1]. As is known to us all, SPPs can break through the diffraction limit and confine the electromagnetic field tightly to metal-dielectric interface. At the same time, novel dispersion characteristics can be obtained by altering the subwavelength scales [2]. Therefore, its potential optical characteristics have attracted much interest in researchers.

However, in lower frequencies such as terahertz and microwave, metals behave equivalently as perfectly electrical conductors (PEC) without negative dielectric constant and simultaneously with extra low skin depth [3], resulting in the metals not supporting the SPPs. To overcome this imperfection, the concept of plasma metamaterials with periodic sub-wavelength grooves or holes structures etched on metal surfaces is proposed [4], which can optimize the dispersion characteristics by altering the geometric parameters of the subwavelength structures. The surface waves similar to SPPs waves generated on the surface of plasma metamaterials is named spoof SPP (SSPPs). Nevertheless, the size of plasma metamaterials cannot be neglected in three dimensional space, which limits the practical application of SSPPs to some extent. Recently, conformal surface plasmon (CSPs) has been reported [5], which can reduce the size of plasma metamaterials and diversify their shapes, thus extending the applications of SSPPs devices.

At present, many SSPPs devices have been reported, such as antennas, filters, power dividers and so on. However, improving the conversion efficiency from traditional waveguides to SSPPs waveguides is quite challenging on all plasma devices. Hence, methods of common guided waves and SSPPs conversion using gratings have been proposed [6]. Whereas the mismatch of momentum of the two waves results in low transmission efficiency and weakens the performance of the device. Recently, plenty of valuable works have been proposed to obtain efficient transition to the coplanar transmission lines (slot line [7], coplanar waveguide [8], [9], and microstrip line [10]) and the SSPPs structure. Momentum matching is achieved perfectly by loading the transition part of the gradient grooves [11], [12], while its lateral dimensions can be further decreased. In addition, gradient-index metasurfaces can be used as transition part to achieve impedance matching efficiently [13], but the further structure simplification is in need. Further research utilizing a transition structure composed of grooves and defects is proposed [14]–[16], which greatly reduces the lateral dimension of the transition from the transmission line to the SSPPs structures. These plasma devices have been reported to have good working characteristics, but for the working wavelength, their size is still larger. The most important factor leading to a larger size is that the transition structure occupies a relatively large scale, which increases the overall size of the device and reduces the integration of the device. It can be seen that it is extremely significant to design and fabricate a filter with simple structure, efficient transition part, and compact size.

In this work, we propose an efficient miniaturized low-pass filter with the novel transition structure. The transition structure is designed with a combination of two inclined rectangular strips and two right-angled triangles. The simple and compact transition structures can perfectly achieve both impedance matching and wave vector matching, simultaneously convert the quasi-TEM waves of the microstrip line to SSPPs waves. More importantly, the proposed transition structure avoids unnecessary electromagnetic leakage and increases radiation efficiency of the low-pass filter. The experiment results agree well with simulation, showing excellent performance of transmission and wideband characteristics. Therefore, this study is of great significance for design and integration of advanced plasma equipment.

II. Filter Design

A. Design and Analysis of SSPPs Unit Cell

One SSPPs unit cell of a miniaturized low-pass filter is shown in Fig. 1(a). Copper is supported by dielectric F4B

Manuscript received June 18, 2019; accepted June 21, 2019. Date of publication June 27, 2019; date of current version July 17, 2019. This work was supported in part by the National Defense Pre-Research Foundation of China under Grant 6140450010302, in part by the Key Research and Development Plan of Shaanxi Province under Grant 2017ZDXM-GY-117, and in part by the Doctoral Innovation Fund of Xi'an University of Technology. *(Corresponding author: Yuchen Zhao.)*

The authors are with the Faculty of Automation and Information Engineering, Xi'an University of Technology, Xi'an 710048, China (e-mail: zhaoyuchen@xaut.edu.cn).

Color versions of one or more of the figures in this letter are available online at http://ieeexplore.ieee.org.

Digital Object Identifier 10.1109/LPT.2019.2925509

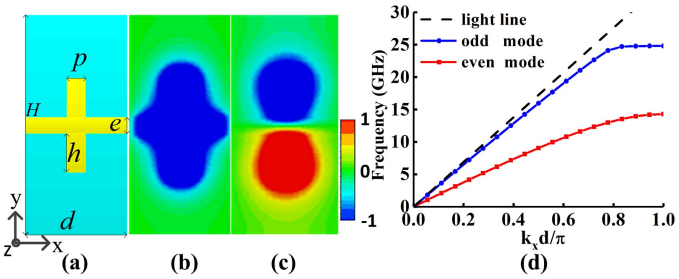

Fig. 1. (a) Schematic diagram of a periodic structure of SSPPs. (b) and (c) are the electric field distribution of the even and odd modes in z-direction, respectively. (d) Dispersion curves for odd mode and even mode of SSPPs.

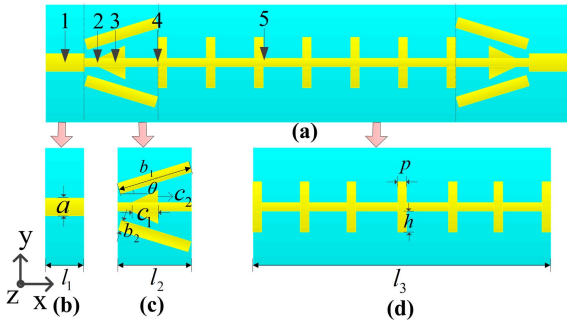

Fig. 2. (a) Top view of the designed miniaturized SSPPs low-pass filter. (b) Microstrip line structure. (c) Transitional structure. (d) Conventional comb SSPPs structure.

with relative dielectric constant $\varepsilon_r = 2.65$ and the loss tangent $\tan\delta = 0.003$, with thickness of metal and dielectric fixed as $t_1 = 0.035$ mm and $t_2 = 0.5$ mm, respectively. For exploring the mode characteristics of SSPPs supported by a unit cell, the distribution of E_Z field is simulated by using the eigenmode solver of the commercial software CST. The x-direction of the unit cell is set to the period boundary, and the scanning angle is increased from 0° to 180°. The electric fields of even mode and odd mode on E_Z component are symmetric distribution (Fig. 1(b)) and antisymmetric distribution (Fig. 1(c)), respectively. It has been confirmed in previous studies that odd mode and even mode exist when electromagnetic waves propagate in symmetric structures [17].

Dispersion curves of the odd and even modes of the proposed miniaturized low-pass filter is simulated, shown in Fig. 1(d), where k_x is the wave vector of x-component in the horizontal direction. The red curve with square marks stands for the dispersion curve of the even mode with an asymptotic frequency of 14.3 GHz and the blue curve with dot marks of the odd mode with an asymptotic frequency of 24.8 GHz. Dispersion curves of both odd and even modes are on the right lower side of the light line. The phenomenon indicates that the propagation of SSPPs waves can be supported by the two modes. In addition, the even mode dispersion curve deviates from the light more significantly than the odd mode dispersion curve, and the corresponding wave vector is larger. In other words, the constraints of even modes on electromagnetic waves are stronger than odd modes in this filter. Furthermore, we know that the fundamental mode of the filter is the even mode, therefore only the characteristic of even mode will be analyzed later.

B. Designed Filter Structure

A top view of the SSPPs low-pass filter with the novel transition structure is shown in Fig. 2(a), the yellow portion is a copper layer, and the blue portion is a dielectric substrate. We know that using the ground plane to design the filter can realize the smooth transition [9] and efficient conversion [5] from traditional microwave transmission lines to SSPPs structures, and can simplify the design of the transition part. Therefore, we also use this ground plane structure to design the filter as shown in Fig. 2(a). For convenient analysis, we divide the filter into microstrip line, novel transitional structure, and conventional SSPPs. Fig. 2(b) shows the microstrip transmission line structure connected to SMA. Fig. 2(c) is a novel transition structure consisting of two rectangular strips having an inclination angle $\theta = 17°$ and

TABLE I
OPTIMIZED VALUE OF FILTER PARAMETERS

Parameter	H	p	e	h	a
Value (mm)	7.47	0.8	0.65	1.6	1.37
Parameter	l_1	l_2	l_3	b_1	b_2
Value (mm)	3.5	6.72	27.08	6.6	0.84
Parameter	c_1	c_2	t_1	t_2	θ
Value (mm)	2.38	0.95	0.035	0.5	17°

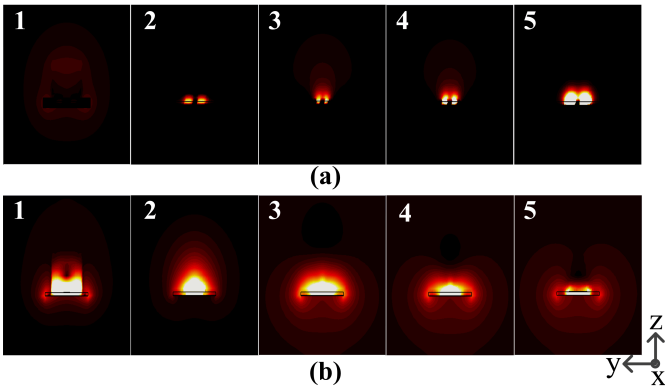

Fig. 3. Electrical field distribution patterns of (a) normal and (b) azimuthal components.

two right-angled triangle patches. It can efficiently convert the quasi-TEM mode in the microstrip line into the SSPPs mode. Fig. 2(d) is a conventional SSPPs structure composed of a plurality of unit cells with height of $h = 1.6$ mm and width of $p = 0.8$ mm, in which the electromagnetic waves is tightly confined to the surface of the SSPPs structure. The optimized values of all parameters of the filter are shown in Table I.

C. Working Mechanism

As we all know, transitional structures designing is the most important part in plasmon filters. It not only realizes impedance matching, but also transforms the quasi-TEM mode in microstrip line into TM-polarized SSPPs mode. In order to observe the process of transitional structure more clearly and intuitively, we simulate the normal ($|E_x|$) and azimuthal ($\sqrt{(|E_y|^2 + |E_z|^2)}$) components of electric field at different positions at 7 GHz. Fig. 3(a) shows the magnitude of the

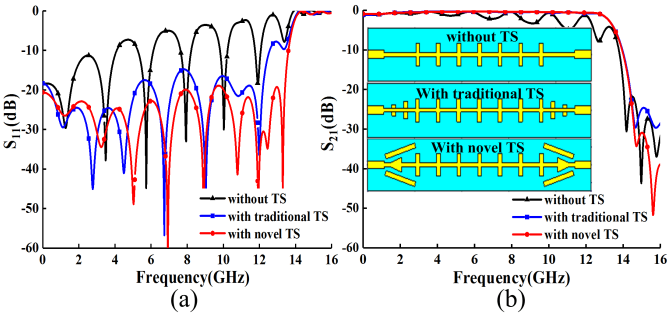

Fig. 4. (a) Reflection coefficients curves of the three filters (without TS, with traditional TS and with novel TS). (b) The curves of the transmission coefficients of the three filters.

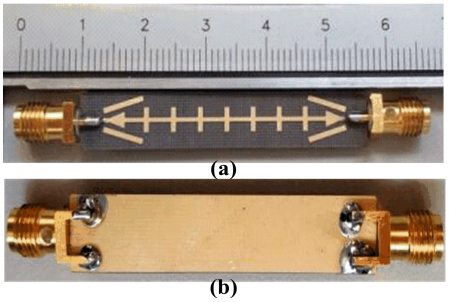

Fig. 5. The (a) front and (b) back photos of the proposed low-pass filter prototype.

normal component of the electric field at five different positions of the filter, corresponding to the plane of the filter at point 1 - 5 in Fig. 2(a). From the plane 1 in Fig. 3(a), we can see that the electric field of normal component on the microstrip line is extremely small and negligible. The main part of the electric field is concentrated on the azimuthal component of plane 1 in Fig. 3(b). With the wave propagating through the region of 2, 3 and 4 of the transition part, the normal component gradually increases while the azimuth component decreases. After the quasi-TEM mode in the microstrip line is converted to SSPPs mode, the main component of the electric field is the normal one, as shown in Fig. 3(a), plane 5. It indicates that the designed transitional structure can efficiently convert the quasi-TEM waves in microstrip lines into SSPPs. At the same time, the transition structure has a prominent advantage that it can make full use of the vertical idle space and reduce the length of the transition structure by 77 %. In addition, the impedance is perfectly matched to 50 ohms, greatly improving the transmission efficiency of the filter.

D. Analysis of Transitional Structure

To demonstrate the necessity of the transition structure (TS), we simulated the reflection and transmission coefficients of the three filters in the inset of Fig. 4(b). Materials and sizes of the dielectric substrates, transmission lines and SSPPs structures of the three filters keep the same for fair comparison. Reflection coefficient (S_{11}) is awfully poor and the bandwidth is less than 4 GHz when no transition structure exists, as shown in Fig. 4(a). After loading the conventional transition structure, reflection coefficient is obviously improved and the bandwidth reaches to 12 GHz. But its disadvantages are that the band-edge selectivity is poor, and the high-frequency performance of the filter is reduced. These shortcomings can be overcome if loading a novel transition structure, as shown by red line in Fig. 4(a). The S_{11} loaded with the novel transition structure is basically lower than -20 dB in the frequency range of 0 - 13 GHz, and the curve at the sideband is steep, showing its better filtering characteristics.

Fig. 4(b) shows a comparison of the S_{21} curves between the aforementioned three structures. Obviously, the filter without the transition structure has an insertion loss of -8.5 dB in the passband and a large fluctuation. For the other two cases, their transmission coefficient curves within the operating bandwidth are substantially reliable, sharing good agreement with each other. When frequency larger than 14 GHz, the out-of-band rejection of the filter loaded with the novel transition structure reaches -30 dB, which is 10 dB better than the other two filters. It can be seen that the design of the transition section from the transmission line to the plasma structure in the design of the plasma filter is essential. A good transition structure can achieve miniaturization while improving filter performance.

III. Results Analysis

For convenient demonstration, we have made a prototype of the filter, such as (a) and (b) in Figs. 5, which are photographs of the front and back of the filter. The yellow part is metallic copper and the black part is F4B dielectric substrate. The S-parameters of the filter can be measured by connecting the vector network analyzer to the SMA welded on the filter, and the results are shown in Fig. 6. The dotted line represents the measurement and the solid line is the result of the simulation. Obviously, the simulated reflection coefficient is almost less than -20 dB in the 0 - 13 GHz frequency range, while the measured one is less than -14 dB. The deviation of experiment and simulation comes from fabrication error, including the filter processing error or the SMA joint welding error. But overall, the experimental results are in good agreement with the numerical simulations. At the same time, the insertion loss of the filter at the center frequency of 6.5 GHz is -0.33 dB, and the out-of-band rejection at a frequency of more than 14 GHz is less than -30 dB. Remarkably, the filter has an excellent shape factor ($K = BW_{-3dB}/BW_{-20dB} = 1.036$), defined as the ratio of -3 dB and -20 dB bandwidth, being closer to the ideal value one and the better the band-edge selectivity. The purple lines are variation of the filter group delay, and its measured value is close to 0.4 ns in the operating bandwidth, and the fluctuation is small (within 0.3 ns). This shows that the filter we designed is reliable.

All the results verify the efficient transmission characteristics and wide operating bandwidth of SSPPs. To gain deeper insight into the propagation characteristics of SSPPs waves, we simulated the electric field distribution of the z-component at the two specific frequencies of 8 GHz and 15 GHz, as shown in Figs. 7(a) and 7(b). The electric field is symmetrically distributed, indicating that the dominant mode in the filter we designed is the even mode. Quasi-TEM waves in the microstrip line are converted to TM-polarized SSPPs and efficiently pass through the entire filter at 8 GHz (Fig. 7(a)). However, the electric field becomes weaker and finally cuts off at 14.3 GHz, as shown in Fig. 7(b), which coincides with the asymptotic frequency of the even mode in Fig. 1(d).

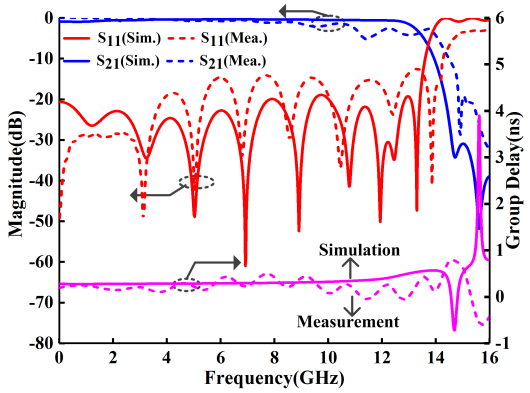

Fig. 6. Experimental and simulation results of S_{11}, S_{21} and group delay.

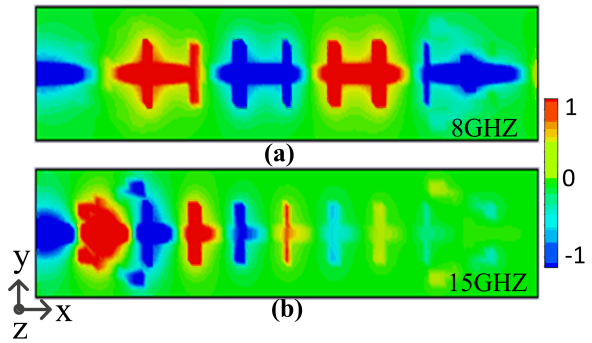

Fig. 7. Electric field distributions of z direction. (a) 8 GHz, (b) 15 GHz.

TABLE II
COMPARISON WITH SOME CURRENTLY ACHIEVED

Ref.	ε_r	Size (mm^2)	Size of TS (mm^2)	BW_{-10dB} (GHz)	Insertion Loss (dB)	Out-of band rejection (dB)
[5]	2.2	140 × 30	52.5 × 24	0 - 11	- 1.7	< -30
[8]	2.65	153 × 43.3	56 × 43.3	0 - 11	-1.7	< -15
[9]	2.65	140 × 50.8	40 × 50.8	0 - 9	-2.3	< -40
[10]	2.65	122 × 2.7	30 × 2.7	0 - 11	-1.7	< -30
This work	2.65	47.52 ×7.47	6.72 ×7.47	0 - 13	-1.2	< -30

In addition, the comparison of the designed filter with other recently published designs is given in Table II. Among them, the width of the model in reference [10] is the smallest, and we find that its optimal width is 2.7 mm (1.5 mm + 2 × 0.6 mm) approximately. The size of our filter is comparable to that of reference [10], and the size of the transition structure (reduced by 38 %) and the overall length of the filter (reduced by 61 %) have been miniaturized. At the same time, the insertion loss and bandwidth of the filter has also been improved. This method provides an idea for the miniaturization of SSPPs filters in the future.

IV. CONCLUSION

In this letter, a miniaturized low-pass SSPPs filter with the novel transition structure is designed and experimentally validated. The designed novel transition structure is composed of two slanted rectangular strips and horizontal right-angled triangular patches, which can efficiently convert the quasi-TEM mode in the microstrip line to the SSPPs mode and achieve wave vector matching and impedance matching. In addition, the mode converter makes full use of the longitudinal space of the filter, which reduces the transverse size of the filter by 61 %, thus realizing the goal of miniaturization of the filter to a certain extent. The numerical simulation and experimental results are in good agreement, which shows that the proposed filter has excellent performance in the microwave band. This study is great significance for the compact integrated system using plasma devices in the microwave band.

REFERENCES

[1] W. L. Barnes, W. A. Murray, J. Dintinger, E. Devaux, and T. W. Ebbesen, "Surface plasmon polaritons and their role in the enhanced transmission of light through periodic arrays of subwavelength holes in a metal film," *Phys. Rev. Lett.*, vol. 92, no. 10, Apr. 2004, Art. no. 107401.
[2] W. L. Barnes, A. Dereux, and T. W. Ebbesen, "Surface plasmon subwavelength optics," *Nature*, vol. 424, no. 6950, p. 824, Aug. 2003.
[3] J. F. O'Hara, R. D. Averitt, and A. J. Taylor, "Terahertz surface plasmon polariton coupling on metallic gratings," *Opt. Express*, vol. 12, no. 25, pp. 6397–6402, Dec. 2004.
[4] T. Jiang, L. Shen, J. J. Wu, T.-J. Yang, Z. Ruan, and L. Ran, "Realization of tightly confined channel plasmon polaritons at low frequencies," *Appl. Phys. Lett.*, vol. 99, no. 26, Dec. 2011, Art. no. 261103.
[5] L. Liu, Z. Li, B. Z. Xu, J. Xu, C. Chen, and C. Gu, "Fishbone-like high-efficiency low-pass plasmonic filter based on double-layered conformal surface plasmons," *Plasmonics*, vol. 12, no. 2, pp. 439–444, Jun. 2017.
[6] Y. Tang, Z. Wang, L. Wosinski, U. Westergren, and S. He, "Highly efficient nonuniform grating coupler for silicon-on-insulator nanophotonic circuits," *Opt. Lett.*, vol. 35, no. 8, pp. 1290–1292, Apr. 2010.
[7] Y. J. Zhou and B. J. Yang, "A 4-way wavelength demultiplexer based on the plasmonic broadband slow wave system," *Opt. Express*, vol. 22, no. 18, pp. 21589–21599, Sep. 2014.
[8] D. Zhang, K. Zhang, Q. Wu, G. Yang, and X. Sha, "High-efficiency broadband excitation and propagation of second-mode spoof surface plasmon polaritons by a complementary structure," *Opt. Lett.*, vol. 42, no. 14, pp. 2766–2769, Jul. 2017.
[9] D. Zhang, K. Zhang, Q. Wu, X. Ding, and X. Sha, "High-efficiency surface plasmonic polariton waveguides with enhanced low-frequency performance in microwave frequencies," *Opt. Express*, vol. 25, no. 3, pp. 2121–2129, Feb. 2017.
[10] D. Zhang, K. Zhang, Q. Wu, R. Dai, and X. Sha, "Broadband high-order mode of spoof surface plasmon polaritons supported by compact complementary structure with high efficiency," *Opt. Lett.*, vol. 43, no. 13, pp. 3176–3179, Jul. 2018.
[11] R. K. Jaiswal, N. Pandit, and N. P. Pathak, "Spoof surface plasmon polaritons based reconfigurable band-pass filter," *IEEE Photon. Technol. Lett.*, vol. 31, no. 3, pp. 218–221, Feb. 1, 2019.
[12] N. Pandit and N. P. Pathak, "Reconfigurable spoof surface plasmon polaritons based band pass filter," in *Proc. IEEE/MTT-S Int. Microw. Symp.*, Jun. 2018, pp. 224–227.
[13] H. F. Ma, X. Shen, Q. Cheng, W. X. Jiang, and T. J. Cui, "Broadband and high-efficiency conversion from guided waves to spoof surface plasmon polaritons," *Laser Photon. Rev.*, vol. 8, no. 1, pp. 146–151, 2014.
[14] A. Kianinejad, Z. N. Chen, and C.-W. Qiu, "Design and modeling of spoof surface plasmon modes-based microwave slow-wave transmission line," *IEEE Trans. Microw. Theory Techn.*, vol. 63, no. 6, pp. 1817–1825, Jun. 2015.
[15] G. Mittal and N. P. Pathak, "Hybrid mode transmission line and band pass filter implementation using plasmonics metamaterial at microwave frequency," in *Proc. ICIIS*, Roorkee, India, Dec. 2016, pp. 207–210.
[16] D. Cao, Y. Li, and J. Wang, "Wideband compact slotline-to-spoof-surface plasmon-polaritons transition for millimeter waves," *IEEE Antennas Wireless Propag Lett.*, vol. 16, pp. 3143–3146, 2017.
[17] X. Liu, Y. Feng, K. Chen, B. Zhu, J. Zhao, and T. Jiang, "Planar surface plasmonic waveguide devices based on symmetric corrugated thin film structures," *Opt. Express*, vol. 22, no. 17, pp. 20107–20116, Aug. 2014.